The Mangotoxin Biosynthetic Operon (*mbo*) Is Specifically Distributed within *Pseudomonas syringae* Genomospecies 1 and Was Acquired Only Once during Evolution

Víctor J. Carrión,[a] José A. Gutiérrez-Barranquero,[a] Eva Arrebola,[b] Leire Bardaji,[c] Juan C. Codina,[a] Antonio de Vicente,[a] Francisco M. Cazorla,[a] Jesús Murillo[c]

Instituto de Hortofruticultura Subtropical y Mediterránea La Mayora (IHSM-UMA-CSIC), Departamento de Microbiología, Facultad de Ciencias, Universidad de Málaga, Málaga, Spain[a]; Instituto de Hortofruticultura Subtropical y Mediterránea La Mayora (IHSMUMA-CSIC), Estación Experimental La Mayora, Algarrobo-Costa, Málaga, Spain[b]; Laboratorio de Patología Vegetal, ETS Ingenieros Agrónomos, Universidad Pública de Navarra, Pamplona, Spain[c]

Mangotoxin production was first described in *Pseudomonas syringae* pv. syringae strains. A phenotypic characterization of 94 *P. syringae* strains was carried out to determine the genetic evolution of the mangotoxin biosynthetic operon (*mbo*). We designed a PCR primer pair specific for the *mbo* operon to examine its distribution within the *P. syringae* complex. These primers amplified a 692-bp DNA fragment from 52 mangotoxin-producing strains and from 7 non-mangotoxin-producing strains that harbor the *mbo* operon, whereas 35 non-mangotoxin-producing strains did not yield any amplification. This, together with the analysis of draft genomes, allowed the identification of the *mbo* operon in five pathovars (pathovars aptata, avellanae, japonica, pisi, and syringae), all of which belong to genomospecies 1, suggesting a limited distribution of the *mbo* genes in the *P. syringae* complex. Phylogenetic analyses using partial sequences from housekeeping genes differentiated three groups within genomospecies 1. All of the strains containing the *mbo* operon clustered in groups I and II, whereas those lacking the operon clustered in group III; however, the relative branching order of these three groups is dependent on the genes used to construct the phylogeny. The *mbo* operon maintains synteny and is inserted in the same genomic location, with high sequence conservation around the insertion point, for all the strains in groups I and II. These data support the idea that the *mbo* operon was acquired horizontally and only once by the ancestor of groups I and II from genomospecies 1 within the *P. syringae* complex.

The bacterial plant pathogen *Pseudomonas syringae* is ubiquitous in nature and often causes economically important plant diseases. This bacterial species establishes an epiphytic population in association with a plant host's surfaces prior to infection. There are at least 50 pathovars, many of which cause a wide range of plant diseases that exhibit diverse symptoms, such as leaf or fruit lesions, cankers, blasts, and galls (1–7).

P. syringae produces several type III effectors and virulence factors, but the role of its toxins is particularly significant during symptom development (1, 8–10). The current study is focused on mangotoxin, which inhibits the enzyme ornithine *N*-acetyltransferase (11, 12). Mangotoxin was initially detected in strains from *P. syringae* pv. syringae (11); however, its production was recently observed in strains of pathovar avellanae (13). Recent studies have reported the involvement of the *mgo* (8, 12, 14) and *mbo* (15) operons in mangotoxin production and *P. syringae* pv. syringae virulence. The *mbo* operon is composed of six genes, and all of them are directly involved in mangotoxin production.

The development of specific methods for pathogen detection *in planta* is very important. In this sense, different PCR methods have been developed and improved to detect different *P. syringae* pathovars. For example, one PCR method used primers that were based on the 16S-23S ribosomal genes to identify strains of *P. syringae* pv. actinidae in which the PCR resulted in a specific amplicon of this pathovar (16). A multiplex PCR assay has been developed for the identification and differentiation of *P. fragi*, *P. lundensis*, and *P. putida* on the basis of the coamplification of different carbamoyl phosphate synthase small-subunit gene fragments (17). Another example is the amplification of the gene *iaaL*, yielding a 454-bp fragment that allows the identification and de-

tection of *P. syringae* pv. savastanoi strains (18). In the current study, we have developed a sensitive and specific method for the detection of mangotoxin-producing strains by a PCR that is based on the amplification of an *mbo* operon region in *P. syringae*. The specificity of the *mbo* operon within mangotoxin biosynthesis was essential for the planning and development of this method (15).

Additionally, the study of specific genes for the biosynthesis and production of virulence factors, as in the case of the *mbo* operon, could also be used in phylogenetic studies. Sawada et al. (19) revealed a remarkable degree of congruence between two housekeeping genes (*gyrB* and *rpoD*) and two components of the pathogenesis-associated type III secretion system (*hrpS* and *hrpL*), leading to the conclusion that the type III secretion system was acquired prior to the diversification of the *P. syringae* pathovars. The diversity of *P. syringae* strains has been further explored by physical mapping of the ribosomal gene cluster, revealing that the size and structure of *P. syringae* genomes vary greatly by pathovar and that large-scale genomic rearrangements are common (20). In this study, a phylogenetic analysis using housekeeping genes has

enabled us to establish a basis for the comparison and study of the *mbo* operon across a group of strains belonging to different pathovars of *P. syringae*. Characterizing the allocation and internal organization of the *mbo* operon has also been realized to obtain information about the evolutionary history of *mbo* genes in the *P. syringae* complex. Moreover, sequencing of the *mbo* operon in four strains belonging to pathovar syringae was carried out to perform a comparison.

MATERIALS AND METHODS

Bacterial strains and growth conditions. The bacterial strains used in this work are described in Table 1. *Escherichia coli* CECT831 (Colección Española de Cultivos Tipo, Spain) was used as the indicator strain for antimetabolite toxin production and was cultured at 37°C using Luria-Bertani medium (41). *P. syringae* was routinely propagated at 28°C using King's medium B (42).

Detection of *P. syringae* antimetabolite toxin production. Antimetabolite toxin production was assayed using the previously described indicator technique (43, 44) that evaluates growth inhibition of *E. coli* on *Pseudomonas* minimal medium (PMS). Briefly, *P. syringae* strains to be assayed were stabbed onto a double layer of the *E. coli* strain CECT831 indicator bacterium and incubated at 22°C for 24 h, followed by an additional 24 h of incubation at 37°C. The production of an antimetabolite toxin was deduced from the appearance of inhibition haloes around the *P. syringae* strains, and the identity of the biochemical step that was inhibited by the antimetabolite toxin was confirmed by reversion of the haloes in separate PMS plates containing 100 μl of a 100 mM solution of the corresponding amino acids, L-glutamate, *N*-acetyl-L-glutamate, *N*-acetyl-ornithine, L-citrulline, and L-arginine (Fig. 1).

General molecular techniques. Standard molecular biology techniques were used for experimentation (41). Genomic DNA was prepared using a Jet-Flex genomic DNA purification kit (Genomed) following the manufacturer's instructions. DNA concentrations and quality were determined with a NanoDrop ND-1000 (NanoDrop Technologies) spectrophotometer and by agarose gel electrophoresis.

DNA sequence analysis and primer design. Multiple-sequence alignments were constructed with the program ALIGN X of the Vector NTI suite (version 9.0; InforMax). Primers for conserved regions of the selected target genes were designed using Primer3 software (45).

PCR amplification was done using Go*Taq* DNA polymerase (Promega); amplification conditions consisted of an initial denaturation step at 94°C for 1 min, followed by 30 cycles of 94°C for 30 s, 52°C for 30 s, and 72°C for 1 min and a final extension step at 72°C for 7 min in a Techne TC-412 thermal cycler. Amplification products were analyzed by agarose gel electrophoresis and stained with ethidium bromide.

The conservation of the *mbo* operon insertion point in different *P. syringae* strains was examined by PCR using primers (mboIS-For/mboIS-Rev; see Table S1 in the supplemental material) that overlapped the right operon border. In the same way, the *mbo* operon synteny was determined using the three primer pairs mboAB-For/mboC-Rev, mboC-For/mboDE-Rev, and mboDE-For/mboF-Rev (see Table S1 in the supplemental material), which amplified overlapping DNA fragments that cover the whole *mbo* operon (see Fig. 7).

Phylogenetic analysis. A phylogenetic analysis based on partial *rpoD* and *gyrB* sequences was done using sequences of *Pseudomonas* spp. that were available in the NCBI database and generated by us from the *P. syringae* strains described in Table 1. Primers rpoDFor2/rpoDRev2 and gyrBFor2/gyrBRev2 (13) or rpoDFor3/rpoDRev3 and gyrBFor3/gyrBRev3 (see Table S1 in the supplemental material) were used for *rpoD* and *gyrB* amplification, and purified amplicons were sequenced by Macrogen. Partial sequences of *rpoD* (807 bp) and *gyrB* (890 bp) were concatenated, resulting in an alignment of 1,697 sites.

Other phylogenetic analyses were done using concatenated partial or complete sequences available in the databases of the housekeeping genes *rpoD* and *gyrB* (4,032 sites) and *gltA*, *pgi*, *recA*, and *rpoD* (5,871 sites); the partial sequence of the *mgoA* gene (2,582 sites), which encodes a nonribosomal peptide synthetase involved in mangotoxin production (12); or the partial sequences of the *mbo* genes, which are involved in mangotoxin biosynthesis (15). Searches for sequence similarity in the NCBI databases were carried out using BLAST algorithms (46). Genome and nucleotide sequences were visualized and manipulated using the Artemis genome browser (47) and compared using the Artemis comparison tool (ACT) (48) in combination with WebACT (49). Concatenated sequences from the same strain were treated as a single sequence; multiple-sequence alignments were done using the Muscle program, and determination of the optimal nucleotide substitution model and phylogenetic tree construction were done using MEGA5 software (50). *P. fluorescens* Pf-5 or *P. syringae* pv. oryzae 1_6 was used as the outgroup. Neighbor-joining, maximum-parsimony, and maximum-likelihood phylogenetic trees of the individual gene sequences and concatenated data sets were generated using MEGA5 with the optimal model parameters and the option of complete deletion to eliminate positions containing gaps. Confidence levels for the branching points were determined using 1,000 bootstrap replicates.

Nucleotide sequence accession numbers. All *gltA*, *gyrB*, *pgi*, *recA*, and *rpoD* gene sequences were deposited in GenBank under accession numbers JX867777 to JX867781, JX867783 to JX867860, JX867862 to JX867932, and JX878889 to JX878894. Sequences of the *mbo* operons and *mgoA* genes were deposited in GenBank under accession numbers JX878400 to JX878403.

RESULTS

Genes for mangotoxin production are restricted to some pathovars of genomospecies 1. Antimetabolite toxin production by the 94 *P. syringae* strains representing 20 pathovars and 6 genomospecies listed in Table 1 was evaluated with an *E. coli in vitro* inhibition assay (43, 44). Mangotoxin production was detected in diverse strains of *P. syringae* pv. avellanae, pisi, and syringae (Table 1), confirming the earlier descriptions of pathovars syringae (11) and avellanae (13) as mangotoxin producers. Three pathovar tomato strains produced an unnamed antimetabolite toxin (Fig. 1) that inhibits the conversion of *N*-acetyl-L-glutamate to *N*-acetyl-ornithine (11, 51). Additionally, strain *P. syringae* pv. syringae ITACyL 488, which was isolated from vetch, produced inhibition haloes in the *E. coli* inhibition test that could not be reverted with any of the tested amino acids. Therefore, this strain might be producing a new toxin with characteristics that remain to be determined.

The phenotypic identification of mangotoxin-producing strains by the *E. coli* inhibition assay is cumbersome and time-consuming. We therefore developed a PCR method to detect strains that harbored the *mbo* operon, which is essential for mangotoxin production (15). Among 20 primer pairs assayed that covered single or adjacent genes of the *mbo* operon, we selected pair mbo24-For/mbo24-Rev (see Table S1 in the supplemental material) to amplify a 692-bp fragment overlapping genes *mboA* and *mboB* because it produced a strong and specific band, with no spurious banding (data not shown). We then detected the presence or absence of the *mbo* operon using primer pair mbo24-For/mbo24-Rev in 94 strains belonging to 20 *P. syringae* pathovars and 6 genomospecies. We obtained a 692-bp specific amplicon for 59 of the analyzed strains, which belonged to 5 pathovars; all of them were part of genomospecies 1 (Fig. 2 and 3; Table 1). However, only 52 of these strains produced mangotoxin in the *E. coli* inhibition test: 4 *P. syringae* pv. aptata strains and 3 *P. syringae* pv. syringae strains (UMAF0167, 1444-5, and FF5) yielded a strong amplification band (Fig. 2) but did not produce mangotoxin.

Additionally, we did not detect a specific amplicon or mango-

TABLE 1 Production of antimetabolite toxins and possession of the *mbo* operon by a collection of *P. syringae* strains

P. syringae pathovar and strain	Host and place of isolation	Source or reference[a]	Antimetabolite toxin produced[b]	*mbo* operon[c] Detection	Insertion site
Cit7[d]*	Orange, USA	Baltrus et al. (21)	ND	+	+
aceris MAFF302273*	Maple, USA	Baltrus et al. (21)	−	−	
actinidae					
NCPPB3738	Kiwi, Japan	Murillo et al. (13)	Phaseolotoxin	−	−
NCPPB3739	Kiwi, Japan	Murillo et al. (13)	Phaseolotoxin	−	−
NCPPB3740	Kiwi, Japan	Murillo et al. (13)	Phaseolotoxin	−	−
NCPPB3871	Kiwi, Italy	Murillo et al. (13)	Phaseolotoxin	−	−
MAFF302091*	Kiwi, Japan	Baltrus et al. (21)	ND	−	−
aesculi					
2250*	Chestnut, UK	Green et al. (22)	ND	−	−
NCPPB3681*	Chestnut, India	Green et al. (22)	ND	−	−
aptata					
DSM50252	Sugar beet, USA	Baltrus et al. (21)	−	+	+
LMG5059	Sugar beet, USA	BCCM/LMG	−	+	+
LMG5532	Sugar beet, Italy	BCCM/LMG	−	+	+
LMG5646	Sugar beet, New Zealand	BCCM/LMG	−	+	+
avellanae					
ISPaVe011	Hazelnut, Italy	Murillo et al. (13)	Mangotoxin	+	+
ISPaVe2056	Hazelnut, Italy	Murillo et al. (13)	Mangotoxin	+	+
coronafaciens					
CECT4389	Oat, Canada	Arrebola et al. (11)	Tabtoxin	−	−
ICMP3113*	Oat, UK	Yamamoto et al. (21)	ND	−	−
glycinea					
A29-2*	Soybean,	Baltrus et al. (21)	ND	−	−
NCPPB2411*	Soybean, New Zealand	Yamamoto et al. (23)	ND	−	−
japonica MAFF301072*	Barley, Japan	Baltrus et al. (21)	ND	+	+
lachrymans					
MAFF301315*	Cucumber, Japan	Baltrus et al. (21)	ND	−	−
MAFF302278*	Cucumber, USA	Baltrus et al. (21)	ND	−	−
maculicola ICMP 3935*	Broccoli, New Zealand	Yamamoto et al. (23)	ND	−	−
mori MAFF301020*	Mulberry, Japan	Baltrus et al. (21)	ND	−	−
morsprunorum MAFF302280*	Plum, Japan	Baltrus et al. (21)	ND	−	−
oryzae 1_6*	Rice, Japan	Reinhardt et al. (24)	ND	−	−
phaseolicola					
1448A	Bean, Ethiopia	Teverson (25)	Phaseolotoxin	−	−
CYL314	Bean, Spain	Rico et al. (26)	−	−	−
pisi					
1704B	Pea, France	Baltrus et al. (21)	Mangotoxin	+	+
HRI203	Pea, New Zealand	Yamamoto et al. (23)	Mangotoxin	+	+
NCPPB1365	Pea, Canada	NCPPB	Mangotoxin	+	+
savastanoi					
NCPPB3335	Olive, France	Pérez-Martínez et al. (27)	−	−	−
NCPPB639*	Olive, Yugoslavia	Yamamoto et al. (23)	ND	−	−
syringae					
7A7	Ornamental pear, USA	Sundin and Bender (28)	−	−	−
7C6	Ornamental pear, USA	G. W. Sundin	Mangotoxin	+	+
7B12	Ornamental pear, USA	G. W. Sundin	−	−	−
7B40	Ornamental pear, USA	Sundin and Bender (28)	Mangotoxin	+	+
7D46	Ornamental pear, USA	G. W. Sundin	−	−	−
7F29	Ornamental pear, USA	Sundin et al. (29)	Mangotoxin	+	+

TABLE 1 (Continued)

P. syringae pathovar and strain	Host and place of isolation	Source or reference[a]	Antimetabolite toxin produced[b]	*mbo* operon[c] Detection	*mbo* operon[c] Insertion site
8B48	Ornamental pear, USA	Sundin et al. (29)	−	−	−
8C32	Ornamental pear, USA	Sundin et al. (29)	Mangotoxin	+	+
8C43	Ornamental pear, USA	Sundin et al. (29)	−	−	−
8F21	Ornamental pear, USA	Sundin et al. (29)	Mangotoxin	+	+
1444-5	Laurel, Spain	Arrebola et al. (11)	−	+	+
1507-7	Hawthorn, Spain	Arrebola et al. (11)	−	−	−
1559-9	Mango, Spain	Arrebola et al. (11)	Mangotoxin	+	+
B728a	Bean, USA	Feil et al. (30)	−	−	−
CECT127	Lilac, UK	CECT	Mangotoxin	+	+
CECT4429	Lilac, UK	CECT	Mangotoxin	+	+
CFBP3388	Vetch, France	Tourte and Manceau (31)	Mangotox./phaseolotox.	+	+
CRD 09-87	Chickling pea, Spain	Martín-Sanz et al. (32)	−	−	−
DAR77787	Mango, Australia	Young (33)	Mangotoxin	+	+
DAR77789	Mango, Australia	Young (33)	Mangotoxin	+	+
EPSMV3	Pear, Spain	Arrebola et al. (11)	−	−	−
EPS17A	Pear, Spain	Arrebola et al. (11)	Mangotoxin	+	+
FF5	Ornamental pear, USA	Sohn et al. (34)	−	+	+
ITACyL 488	Vetch, Spain	Martín-Sanz et al. (35)	Unknown	−	−
ITACyL 522	Chickling pea, Spain	Martín-Sanz et al. (32)	−	−	−
ITACyL 523	Chickling pea, Spain	Martín-Sanz et al. (32)	−	−	−
ITACyL 524	Chickling pea, Spain	Martín-Sanz et al. (32)	−	−	−
ITACyL 525	Chickling pea, Spain	Martín-Sanz et al. (32)	−	−	−
ITACyL 526	Grass pea, Spain	Martín-Sanz et al. (32)	−	−	−
ITACyL 527	Grass pea, Spain	Martín-Sanz et al. (32)	−	−	−
ITACyL 528	Grass pea, Spain	Martín-Sanz et al. (32)	−	−	−
ITACyL 529	Vetch, Spain	Martín-Sanz et al. (32)	−	−	−
NCPPB1239	Bean, Kenya	NCPPB	Mangotoxin	+	+
Ps-5	Mango, Israel	UMA-LC	Mangotoxin	+	+
Ps-6	Mango, Israel	Arrebola et al. (11)	Mangotoxin	+	+
Ps-10	Mango, Israel	Arrebola et al. (11)	Mangotoxin	+	+
Ps-35	Mango, Israel	Arrebola et al. (11)	Mangotoxin	+	+
UMAF0049	Mango, Spain	Cazorla et al. (36)	Mangotoxin	+	+
UMAF0081	Mango, Spain	Cazorla et al. (36)	Mangotoxin	+	+
UMAF0158	Mango, Spain	Cazorla et al. (36)	Mangotoxin	+	+
UMAF0167	Mango, Spain	Cazorla et al. (36)	−	+	+
UMAF0170	Mango, Spain	Cazorla et al. (36)	Mangotoxin	+	+
UMAF0176	Mango, Spain	Arrebola et al. (11)	Mangotoxin	+	+
UMAF0209	Mango, Spain	UMA-LC	Mangotoxin	+	+
UMAF0214	Mango, Spain	UMA-LC	Mangotoxin	+	+
UMAF0217	Mango, Spain	UMA-LC	Mangotoxin	+	+
UMAF0220	Mango, Spain	UMA-LC	Mangotoxin	+	+
UMAF0221	Mango, Spain	UMA-LC	Mangotoxin	+	+
UMAF0222	Mango, Spain	UMA-LC	Mangotoxin	+	+
UMAF0223	Mango, Spain	UMA-LC	Mangotoxin	+	+
UMAF0225	Mango, Spain	UMA-LC	Mangotoxin	+	+
UMAF0226	Mango, Spain	UMA-LC	Mangotoxin	+	+
UMAF1003	Mango, Spain	Arrebola et al. (11)	Mangotoxin	+	+
UMAF1060	Mango, Spain	Gutiérrez-Barranquero et al. (37)	Mangotoxin	+	+
UMAF2007	Mango, Portugal	Arrebola et al. (11)	Mangotoxin	+	+
UMAF2008	Mango, Portugal	UMA-LC	Mangotoxin	+	+
UMAF2025	Mango, Portugal	Cazorla et al. (36)	Mangotoxin	+	+
UMAF2026	Mango, Portugal	Cazorla et al. (36)	Mangotoxin	+	+
UMAF2676	Bean, South Africa	Arrebola et al. (11)	−	−	−
UMAF2700	Mango, Italy	UMA-LC	Mangotoxin	+	+
UMAF2702	Mango, Italy	Gutiérrez-Barranquero et al. (37)	Mangotoxin	+	+
UMAF2801	Mango, Spain	Gutiérrez-Barranquero et al. (37)	Mangotoxin	+	+
UMAF2802	Mango, Spain	Gutiérrez-Barranquero et al. (37)	Mangotoxin	+	+
UMAF2805	Mango, Spain	UMA-LC	Mangotoxin	+	+
UMAF2808	Mango, Spain	UMA-LC	Mangotoxin	+	+
UMAF2811	Mango, Spain	UMA-LC	Mangotoxin	+	+

(Continued on following page)

TABLE 1 (Continued)

P. syringae pathovar and strain	Host and place of isolation	Source or reference[a]	Antimetabolite toxin produced[b]	*mbo* operon[c] Detection	*mbo* operon[c] Insertion site
UMAF3028	Mango, Spain	Arrebola et al. (11)	Mangotoxin	+	+
UMAF4002	Tomato, Spain	Arrebola et al. (11)	Mangotoxin	+	+
UMAF6024	Purple phlomis, Spain	UMA-LC	Mangotoxin	+	+
UMAF6016	Chestnut, Spain	Arrebola et al. (11)	−	−	−
UMAF6582	Peach, Spain	Arrebola et al. (11)	−	−	−
tabaci ATCC 11528	Tobacco, USA	ATCC	Tabtoxin	−	−
tagetis CECT4430	Marigold, Zimbabwe	CECT	−	−	−
tomato					
DC3000	Tomato, UK	Moore et al. (38)	−	−	−
DCT6D1	Tomato, Canada	Moore et al. (38)	Unnamed	−	−
K40*	Tomato, USA	Cai et al. (39)	ND	−	−
NCPPB1108*	Tomato, UK	Cai et al. (39)	ND	−	−
T1*	Tomato, Canada	Almeida et al. (40)	ND	−	−
UMAF4007	Tomato, Spain	Arrebola et al. (11)	Unnamed	−	−
UMAF6018	Tomato, Spain	Arrebola et al. (11)	Unnamed	−	−

[a] ATCC, American Type Culture Collection; CECT, Colección Española de Cultivos Tipo, Spain; CFBP, Collection Française de Bactéries Associées aux Plantes, France; DSM, German Collection of Microorganisms and Cell Cultures, Germany; BCCM/LMG, Belgian Coordinated Collections of Microorganisms, Belgium; NCPPB, National Collection of Plant Pathogenic Bacteria, United Kingdom; ICMP, International Collection of Microorganisms from Plants, New Zealand; MAFF, Ministry of Agriculture, Forestry and Fisheries, Japan; UMA-LC, IHSM-UMA-CSIC, University of Málaga, Microbiology and Plant Pathology Laboratory Collection.
[b] ND, not determined; −, antimetabolite toxins not detected; Mangotox./phaseolotox., mangotoxin/phaseolotoxin.
[c] The presence or absence (+ and −, respectively) of the *mbo* operon was determined by specific PCR amplification or from bioinformatic analyses of the published genomes from the NCBI (strains marked *); the operon was in all cases inserted in the same genomic location as in strain *P. syringae* pv. syringae UMAF0158.
[d] No pathovar designation.

toxin production in 35 strains (Fig. 2b; Table 1) belonging to the pathovars actinidae ($n = 4$), coronafaciens ($n = 1$), phaseolicola ($n = 2$), savastanoi ($n = 1$), syringae ($n = 21$), tabaci ($n = 1$), tagetis ($n = 1$), and tomato ($n = 4$). Furthermore, a BLAST search of sequenced *P. syringae* genomes belonging to 17 pathovars (http://www.pseudomonas-syringae.org/) (21) revealed the presence of the *mbo* operon in strains Cit7 (without pathovar assignation) and MAFF301072 (*P. syringae* pv. japonica).

In summary, the characterization of a large collection of *P. syringae* strains belonging to 20 pathovars (Table 1) by phenotypic assays, PCR amplification, and/or analysis of their sequenced genomes disclosed the presence of the *mbo* operon for mangotoxin

biosynthesis in strains from five pathovars (pathovars aptata, avellanae, japonica, pisi, and syringae), all of which belong to genomospecies 1 (52).

Elucidation of the *mbo* operon evolutionary history. To study the *mbo* operon evolutionary history within the *P. syringae* complex, we examined the phylogeny of diverse strains using concatenated sequences of internal fragments of housekeeping genes *rpoD* and *gyrB* (total, 1,697 sites). Trees obtained by diverse clustering methods showed the same topology (Fig. 3 and 4a; see Fig. S1 in the supplemental material), and the strains of genomospecies 1 were clustered in three groups within all trees, two of which contained all of the strains harboring the *mbo* operon. Among the
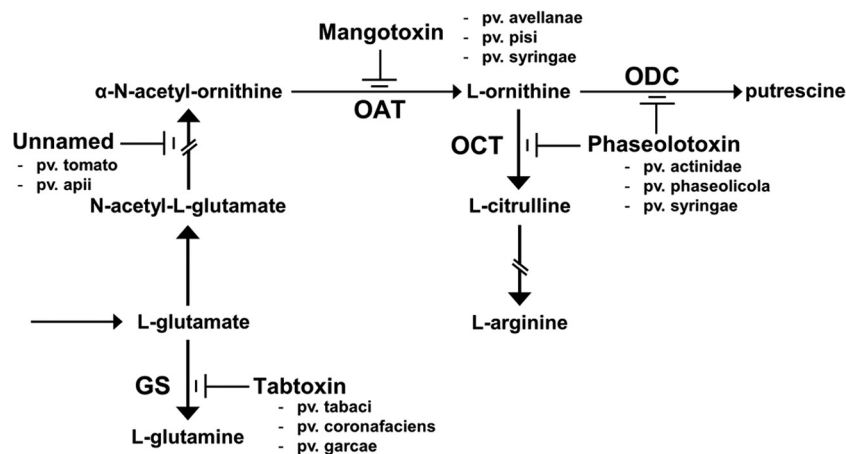

FIG 1 Schematic representation of the arginine-glutamine and polyamine biosynthesis pathways. The enzymatic targets that are inhibited by antimetabolite toxins mangotoxin, phaseolotoxin, tabtoxin, and an unnamed phytotoxin that was produced by different *P. syringae* pathovars are shown. Target enzymes have the following abbreviations: GS, glutamine synthetase; OAT, ornithine *N*-acetyltransferase; OCT, ornithine carbamoyltransferase; and ODC, ornithine decarboxylase. The pathovars of *P. syringae* producing each toxin are indicated.
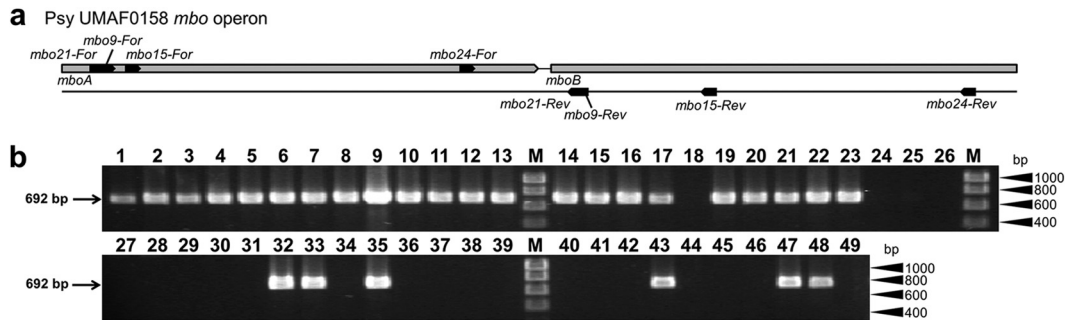
FIG 2 Detection by PCR of a specific mangotoxin biosynthesis operon sequence in different *P. syringae* genomospecies 1 strains. (a) Schematic representation of the four primer pairs designed for *mbo* operon detection in *P. syringae* strains. (b) Gel electrophoresis showing the specific 692-bp product generated with primers mbo24-For and mbo24-Rev from strains harboring the *mbo* operon. Lanes correspond to the following: 1, *P. syringae* pv. syringae 7C67; 2, *P. syringae* pv. syringae 7F29; 3, *P. syringae* pv. syringae 8F21; 4, *P. syringae* pv. syringae 1559-9; 5, *P. syringae* pv. syringae CECT127; 6, *P. syringae* pv. syringae CECT4429; 7, *P. syringae* pv. syringae CFBP3388; 8, *P. syringae* pv. syringae DAR77787; 9, *P. syringae* pv. syringae DAR77789; 10, *P. syringae* pv. syringae EPS17A; 11, *P. syringae* pv. syringae NCPPB1239; 12, *P. syringae* pv. syringae Ps-5; 13, *P. syringae* pv. syringae UMAF0081; 14, *P. syringae* pv. syringae UMAF0214; 15, *P. syringae* pv. syringae UMAF0225; 16, *P. syringae* pv. syringae UMAF1060; 17, *P. syringae* pv. syringae UMAF6024; 18, *P. syringae* pv. syringae UMAF6016; 19, *P. syringae* pv. pisi 1704B; 20, *P. syringae* pv. pisi HRI203; 21, *P. syringae* pv. pisi NCPPB1365; 22, *P. syringae* pv. avellanae ISPaVe011; 23, *P. syringae* pv. avellanae ISPaVe2056; 24, *P. syringae* pv. syringae 7D46; 25, 8B48; 26, *P. syringae* pv. syringae 8C43; 27, *P. syringae* pv. syringae ITACyL 488; 28, *P. syringae* pv. syringae ITACyL 521; 29, *P. syringae* pv. syringae ITACyL 523; 30, *P. syringae* pv. syringae ITACyL 526; 31, *P. syringae* pv. syringae ITACyL 529; 32, *P. syringae* pv. syringae 1444-5; 33, *P. syringae* pv. syringae FF5; 34, *P. syringae* pv. syringae EPSMV3; 35, *P. syringae* pv. syringae UMAF0167; 36, *P. syringae* pv. tomato DC3000; 37, *P. syringae* pv. tomato DCT6D1; 38, *P. syringae* pv. tomato UMAF4007; 39, *P. syringae* pv. tomato UMAF6018; 40, *P. syringae* pv. coronafaciens CECT4389; 41, *P. syringae* pv. phaseolicola 1448A; 42, *P. syringae* pv. phaseolicola CYL314; 43, *P. syringae* pv. aptata DSM50252; 44, *P. syringae* pv. syringae 1507-7; 45, *P. syringae* pv. syringae B728a; 46, *P. syringae* pv. syringae CECT4430; 47, *P. syringae* pv. syringae 0049; 48, *P. syringae* pv. syringae UMAF0158; 49, *P. syringae* pv. tabaci ATCC 11528; M, molecular size marker (HyperLadder I; Bioline).

mangotoxin-producing strains, group I contained 45 strains of *P. syringae* pv. syringae, which were isolated from woody hosts, mainly mangoes, whereas group II contained 16 strains from the pathovars aptata, avellanae, japonica, pisi, and syringae, which were isolated from diverse woody and herbaceous hosts. Group III clustered all the strains from genomospecies 1 that did not contain the *mbo* operon, which included 1 pathovar aceris strain plus 21 pathovar syringae strains. Finally, the remaining strains comprised 30 non-mangotoxin producers from different genomospecies that clustered separately. In this phylogenetic analysis, group III diverged after the separation of groups I and II, suggesting that the *mbo* operon was acquired once by the common ancestor of groups I, II, and III and later lost in group III. An alternative explanation is that the *mbo* operon was acquired independently by the putative ancestors of groups I and II (Fig. 3 and 4a; see Fig. S1 in the supplemental material). To confirm this result, we performed further phylogenetic analyses using additional housekeeping genes (Fig. 4b to d). For these analyses, we used only those strains with an available genome sequence plus two pathovar syringae strains representative of group I (UMAF0158) and group II (CFBP3388).

In the different trees that were built using concatenated sequences of the *gltA*, *pgi*, *recA*, and *rpoD* genes (5,871 sites), a partial sequence of the *mgoA* gene (2,582 sites), or the *mbo* genes (5,114 sites), all strains clustered as in the *gyrB-rpoD* phylogenetic tree. However, and in contrast to the *gyrB-rpoD* tree, group III diverged before the separation of groups I and II. Because this topology has strong bootstrap support, the multilocus sequence typing and *mgoA* trees suggest that the *mbo* operon was acquired by groups I and II in either one or two separate acquisition events and after their separation from group III.

The *mbo* operon is highly conserved among the two phylogroups. Phylogenetic analyses clearly indicated that the strains harboring the *mbo* operon cluster in two well-separated phylo-

groups, groups I and II (Fig. 3 and 4; see Fig. S1 in the supplemental material). We therefore examined whether the operon is conserved in organization, sequence, and physical location in both phylogroups in order to gain support for one of the possible scenarios explaining the evolutionary history of the *mbo* operon.

To further evaluate the conservation of the *mbo* operon in the two phylogroups, we obtained the complete sequence of this operon from *P. syringae* pv. syringae strains UMAF0158, UMAF0167 (both group I), and CFBP3388 (group II) (see Table S2 in the supplemental material) and compared them with the sequence of the operon from the draft genome sequence of strains *P. syringae* Cit7 (group I), and *P. syringae* pv. aptata DSM50252, pisi 1704B, and syringae FF5 (the last three strains are from group II) (see Table S2 in the supplemental material). Sequence analysis of the seven strains reveals that the *mbo* operon maintains synteny and is generally well conserved, ranging in size from 6,769 to 6,801 bp. The operon harbors six open reading frames (ORFs) and shows a 55 to 56% G+C content, which is lower than the average G+C content of the *P. syringae* pv. syringae B728a chromosome (59.23%) (30, 53). The *mbo* operon is highly conserved among strains of group I, with nucleotide identity values being higher than 99%; however, the nucleotide identity among strains of group II varies between 96.5 and 98.5%, which is not surprising, given that this group includes strains from different pathovars. Nevertheless, the *mbo* operon is well conserved when both groups are compared, with levels of nucleotide identity being higher than 94.2% in pair comparisons (see Table S2 in the supplemental material).

We examined the *mbo* operon point of insertion by PCR using a primer pair that overlaps the right border of the operon (Fig. 5). The amplification of DNA from 19 strains from group I and 15 strains from group II produced an amplicon of the same size for all strains (692 bp), whereas no amplification was observed for strains belonging to group III (Fig. 5). Additionally, the compar-
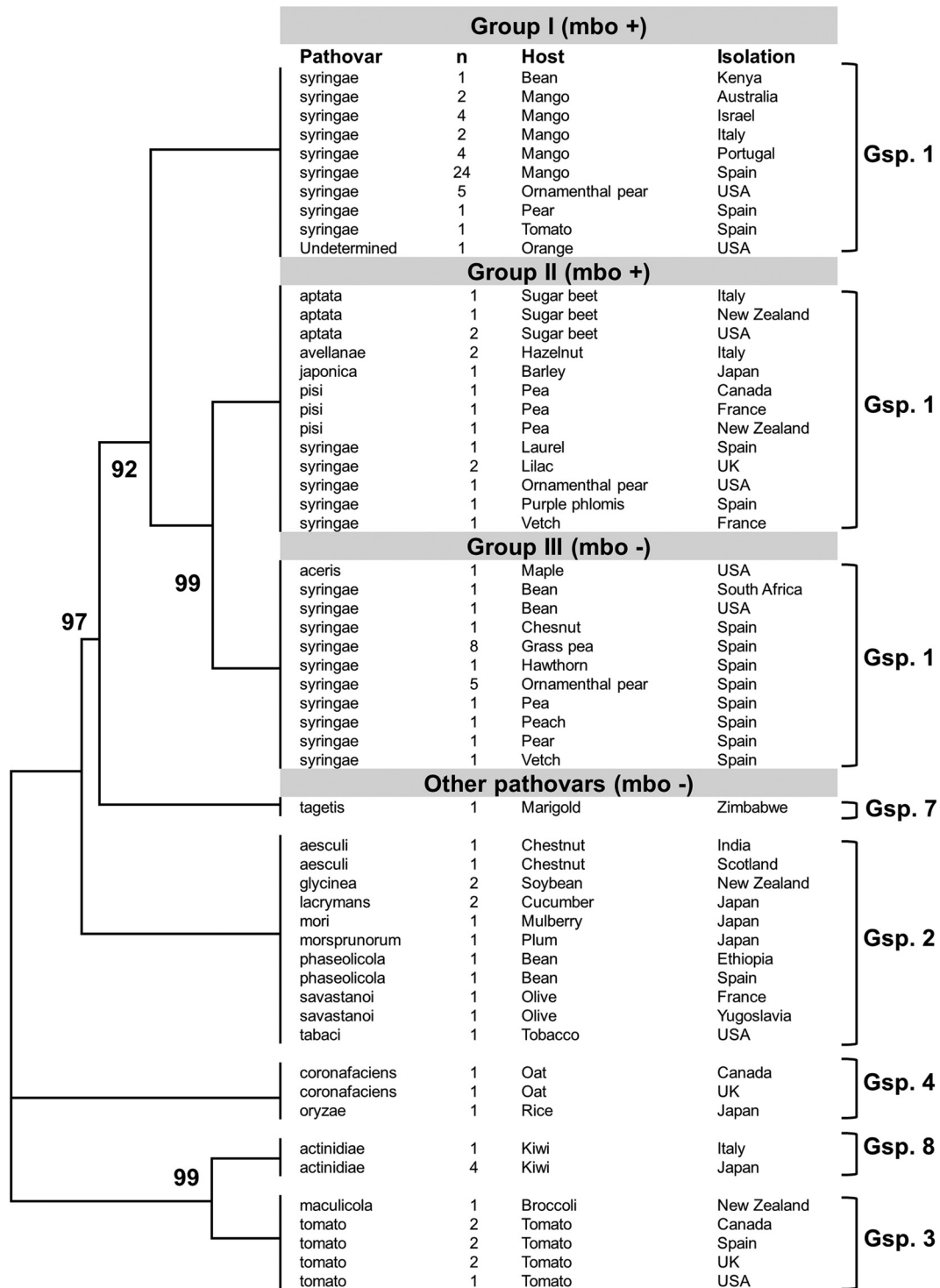
Group I (mbo +)			
Pathovar	**n**	**Host**	**Isolation**
syringae	1	Bean	Kenya
syringae	2	Mango	Australia
syringae	4	Mango	Israel
syringae	2	Mango	Italy
syringae	4	Mango	Portugal
syringae	24	Mango	Spain
syringae	5	Ornamenthal pear	USA
syringae	1	Pear	Spain
syringae	1	Tomato	Spain
Undetermined	1	Orange	USA

Gsp. 1

Group II (mbo +)			
aptata	1	Sugar beet	Italy
aptata	1	Sugar beet	New Zealand
aptata	2	Sugar beet	USA
avellanae	2	Hazelnut	Italy
japonica	1	Barley	Japan
pisi	1	Pea	Canada
pisi	1	Pea	France
pisi	1	Pea	New Zealand
syringae	1	Laurel	Spain
syringae	2	Lilac	UK
syringae	1	Ornamenthal pear	USA
syringae	1	Purple phlomis	Spain
syringae	1	Vetch	France

Gsp. 1

Group III (mbo -)			
aceris	1	Maple	USA
syringae	1	Bean	South Africa
syringae	1	Bean	USA
syringae	1	Chesnut	Spain
syringae	8	Grass pea	Spain
syringae	1	Hawthorn	Spain
syringae	5	Ornamenthal pear	Spain
syringae	1	Pea	Spain
syringae	1	Peach	Spain
syringae	1	Pear	Spain
syringae	1	Vetch	Spain

Gsp. 1

Other pathovars (mbo -)			
tagetis	1	Marigold	Zimbabwe

Gsp. 7

aesculi	1	Chestnut	India
aesculi	1	Chestnut	Scotland
glycinea	2	Soybean	New Zealand
lacrymans	2	Cucumber	Japan
mori	1	Mulberry	Japan
morsprunorum	1	Plum	Japan
phaseolicola	1	Bean	Ethiopia
phaseolicola	1	Bean	Spain
savastanoi	1	Olive	France
savastanoi	1	Olive	Yugoslavia
tabaci	1	Tobacco	USA

Gsp. 2

coronafaciens	1	Oat	Canada
coronafaciens	1	Oat	UK
oryzae	1	Rice	Japan

Gsp. 4

actinidiae	1	Kiwi	Italy
actinidiae	4	Kiwi	Japan

Gsp. 8

maculicola	1	Broccoli	New Zealand
tomato	2	Tomato	Canada
tomato	2	Tomato	Spain
tomato	2	Tomato	UK
tomato	1	Tomato	USA

Gsp. 3

Bootstrap values: 97, 92, 99, 99

FIG 3 Schematic neighbor-joining tree of *P. syringae* strains belonging to different pathovars and harboring or not the *mbo* genes (*mbo* + and *mbo* −, respectively) for mangotoxin production. The neighbor-joining tree was constructed with MEGA5 using the concatenated partial sequences of *rpoD* and *gyrB*. The Tamura-Nei substitution model with gamma correction was used for tree construction. Bootstrap values (1,000 repetitions) are shown on each branch. One hundred thirteen strains of different *P. syringae* pathovars were analyzed. The pathovar, host, and country of isolation are presented on the right, together with the number of strains (indicated by *n*) and the genomospecies (Gsp.) to which they belong, according to Gardan et al. (52). Evolutionary distances are given in units of nucleotide substitutions per site. The topology was similar among trees produced by the maximum-parsimony and maximum-likelihood methods. Sequences of *rpoD* and *gyrB* were extracted from published genome sequences or were sequenced for this work. For more detailed information, see Fig. S1 in the supplemental material.
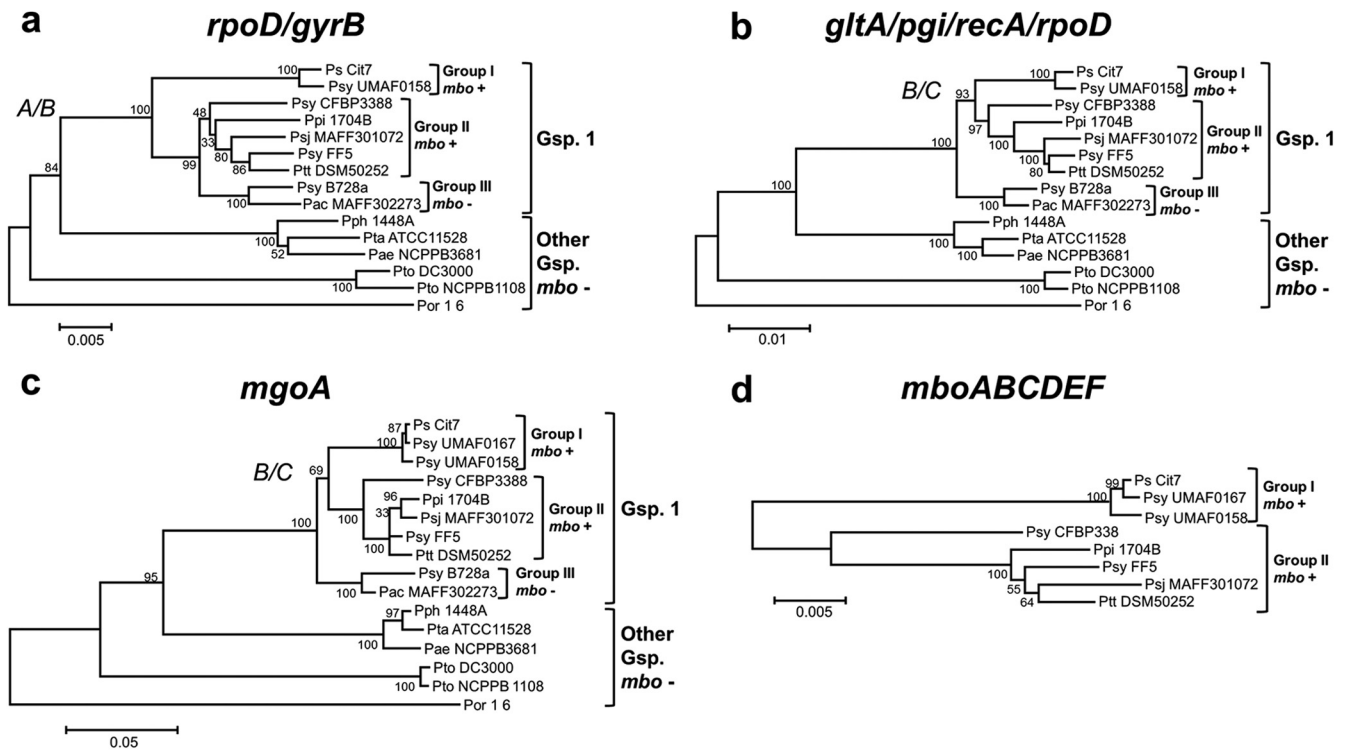
FIG 4 Phylogeny of toxigenic and nontoxigenic *P. syringae* pv. syringae strains using diverse nucleotide sequences. Neighbor-joining trees were constructed with MEGA5 using the concatenated complete sequences of *rpoD* and *gyrB* (a), concatenated partial sequences of *gltA*, *pgi*, *recA*, and *rpoD* (b), a partial sequence of gene *mgoA* (c), and concatenated partial sequences of the *mboABCDEF* genes (d); the substitution models Tamura 3-parameter (*mgoA* and *mbo* genes) and Tamura-Nei (other genes) with gamma correction, as indicated by the model analysis module of MEGA5, were employed. Bootstrap values (1,000 repetitions) are shown on branches. The *mbo* operon acquisition alternatives are marked as follows: A, *mbo* operon acquisition by the common ancestor of groups I, II, and III and loss in group III; B, *mbo* operon acquisition twice independently by groups I and II; C, *mbo* operon acquisition by the common ancestor of groups I and II. *P. syringae* pathovars are abbreviated as follows: Ps, *P. syringae* (no pathovar assigned); Pac, *P. syringae* pv. aceris; Pae, *P. syringae* pv. aesculi; Ptt, *P. syringae* pv. aptata; Psj, *P. syringae* pv. japonica; Ppi, *P. syringae* pv. pisi; Pph, *P. syringae* pv. phaseolicola; Psy, *P. syringae* pv. syringae; Pta, *P. syringae* pv. tabaci; Pto, *P. syringae* pv. tomato; Por, *P. syringae* pv. oryzae. The trees were rooted with *P. syringae* pv. oryzae 1_6. Evolutionary distances are given in units of number of nucleotide substitutions per site. The topology was similar for trees produced by the maximum-parsimony and maximum-likelihood methods. Sequences from some strains were extracted from published genome sequences.

ison of the *mbo* operon sequence from the seven strains indicated above (see Table S2 in the supplemental material) showed that the operon was inserted in the same location in strains from both groups I and II. A comparison of the nucleotide sequences from mangotoxin-producing and non-mangotoxin-producing strains indicates that the insertion of the *mbo* operon is correlated with the loss of a highly conserved 67- or 68-bp sequence (Fig. 6). This sequence is present in the closed genome sequences of *P. syringae* pv. phaseolicola 1448A, *P. syringae* pv. syringae B728a, and *P. syringae* pv. tomato DC3000 (Fig. 6) and is also conserved in sequence and position within the genomes of other *P. syringae* and *P. fluorescens* strains that do not produce mangotoxin (data not shown), indicating that this small fragment is ancestral to *P. syringae* and has been lost during the acquisition of the *mbo* operon. This evidence suggests that the *mbo* operon has never been acquired by strains from group III, which contain the 67-bp fragment.

Finally, the internal organization of the *mbo* operon was determined by PCR using three pairs of primers that produced overlapping amplicons. These primers yielded identical amplification products for all the analyzed strains from groups I and II (Fig. 7), indicating a widely conserved synteny. All of these data showed

that the *mbo* operon was acquired only once during the evolutionary history of *P. syringae*, by a common ancestor of groups I and II.

DISCUSSION

In previous studies by our group, the production of mangotoxin was shown to be associated with *P. syringae* pv. syringae and to contribute to its virulence in tomato plants (8, 11). Recently, Murillo et al. (13) reported the production of mangotoxin by strains of pathovar avellanae, as well as the simultaneous production of two antimetabolite toxins, mangotoxin and phaseolotoxin, by strain *P. syringae* pv. syringae CFBP3388. In the current study, we evaluated the production of mangotoxin and other antimetabolite toxins in 94 strains belonging to different pathovars of the *P. syringae* complex. Besides pathovars avellanae and syringae, we detected production of mangotoxin in three strains of pathovar pisi, which is in contrast to previous analyses that did not find toxin-producing strains in the last pathovar (44, 51). This discrepancy could be due to several reasons, including differential analysis conditions that could impact toxin production; an inherent inability of previously analyzed strains to produce mangotoxin, in spite of having the biosynthesis genes, as we observed with strain FF5; or, since we examined here strains from only one of the two *P.*
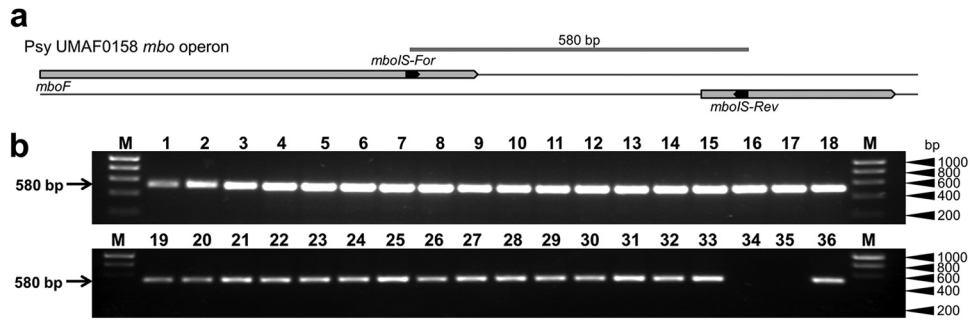
FIG 5 Mapping of the *mbo* operon insertion point in *P. syringae* strains. (a) Schematic representation of the PCR amplification strategy for the 3′ end of the *mbo* operon. Primers mboIS-For/mboIS-Rev (amplicon of 580-bp) were designed between the 3′ end of the *mboF* gene and the next ORF downstream of the *mbo* operon. (b) Representative results of amplification using 34 strains that harbor the *mbo* operon and two non-mangotoxin-producing strains that were used as negative controls. Lanes correspond to the following: 1, *P. syringae* pv. aptata DSM50252; 2, *P. syringae* pv. aptata LMG5059; 3, *P. syringae* pv. aptata LMG5532; 4, *P. syringae* pv. aptata LMG5646; 5, *P. syringae* pv. avellanae ISPaVe011; 6, *P. syringae* pv. avellanae ISPaVe2056; 7, *P. syringae* pv. pisi HRI203; 8, *P. syringae* pv. pisi NCPPB1365; 9, *P. syringae* pv. pisi 1704B; 10, *P. syringae* pv. syringae 7C6; 11, *P. syringae* pv. syringae 7B40; 12, *P. syringae* pv. syringae 7F29; 13, *P. syringae* pv. syringae 1444-5; 14, *P. syringae* pv. syringae 1559-9; 15, *P. syringae* pv. syringae CECT127; 16, *P. syringae* pv. syringae CECT4429; 17, *P. syringae* pv. syringae CFBP3388; 18, *P. syringae* pv. syringae DAR77787; 19, *P. syringae* pv. syringae EPS17A; 20, *P. syringae* pv. syringae FF5; 21, *P. syringae* pv. syringae NCPPB1239; 22, *P. syringae* pv. syringae Ps-10; 23, *P. syringae* pv. syringae UMAF0049; 24, *P. syringae* pv. syringae UMAF0081; 25, *P. syringae* pv. syringae UMAF0167; 26, *P. syringae* pv. syringae UMAF0209; 27, *P. syringae* pv. syringae UMAF0221; 28, *P. syringae* pv. syringae UMAF1060; 29, *P. syringae* pv. syringae UMAF2008; 30, *P. syringae* pv. syringae UMAF2700; 31, *P. syringae* pv. syringae UMAF2802; 32, *P. syringae* pv. syringae UMAF4002; 33, *P. syringae* pv. syringae UMAF6024; 34, *P. syringae* pv. phaseolicola 1448A; 35, *P. syringae* pv. syringae B728a; 36, *P. syringae* pv. syringae UMAF0158; M, molecular size marker (HyperLadder I, Bioline).

syringae pv. pisi lineages (54), the possibility that the previously analyzed strains belong to a phylogenetic lineage that does not produce toxins.

We designed a primer pair specific for the *mbo* operon that was used to screen a collection of 94 strains from 20 *P. syringae* pathovars. The primers were highly specific, yielding amplification only in strains that produced mangotoxin in an *in vivo* inhibition test or in strains that contained the *mbo* operon, confirming the usefulness of this primer pair. All of the strains isolated from lesions of apical necrosis of mango so far have been shown to produce mangotoxin during the inhibition bioassay (11, 55), supporting the idea that this primer pair could potentially be used for the detection of *P. syringae* pv. syringae in mango plants and for broader disease diagnosis. The PCR and the inhibition analyses,

combined with the search for mangotoxin biosynthesis genes in the *P. syringae* genomes from the databases, allowed us to determine that the mangotoxin biosynthesis operon is present only in strains from *P. syringae* pv. aptata, avellanae, japonica, pisi, and syringae, all of which belong to genomospecies 1. The amplification of overlapping DNA fragments as well as the sequence comparisons showed that the composition, structure, and sequence of the *mbo* operon are highly conserved in all these pathovars. Although *P. syringae* pv. syringae FF5, UMAF0167, and UMAF1444-5 and the four *P. syringae* pv. aptata strains yielded the expected amplification products for the *mbo* operon or contained the *mbo* operon in their genome sequence, we did not detect production of mangotoxin in the *in vivo* inhibition test for any of the strains. This is in contrast to a previous report showing
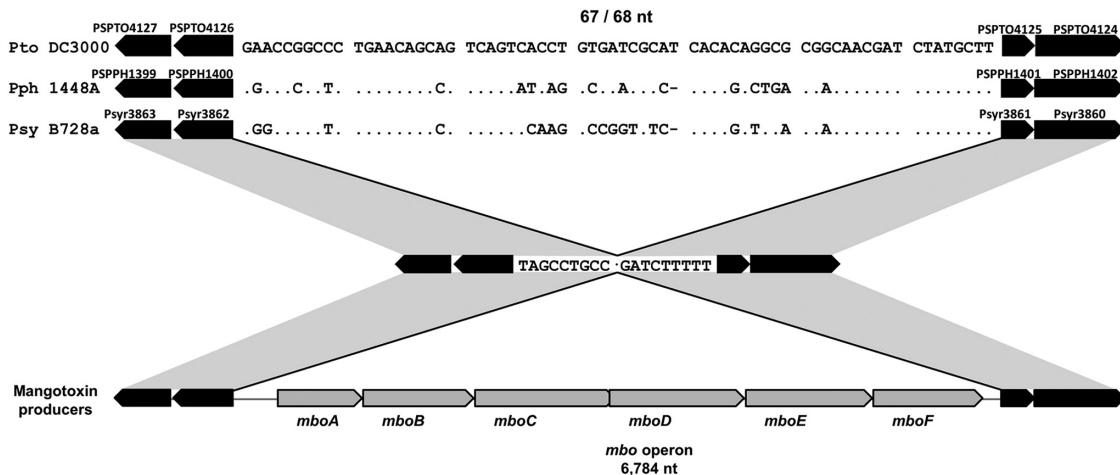

FIG 6 *mbo* operon insertion site analysis. Alignment of the nucleotide sequences bordering the *mbo* operon with the corresponding sequences in non-mangotoxin-producing strains (*P. syringae* pv. phaseolicola 1448A, *P. syringae* pv. syringae B728a, and *P. syringae* pv. tomato DC3000). The nucleotide differences with respect to strain DC3000 are indicated, while dots indicate identical nucleotides and a hyphen shows an indel. The CDSs flanking the point of insertion of the *mbo* operon are shown in black, with indication of their locus tag numbers in the genomes of *P. syringae* pv. tomato DC3000, *P. syringae* pv. phaseolicola 1448A, and *P. syringae* pv. syringae B728a. nt, nucleotides.
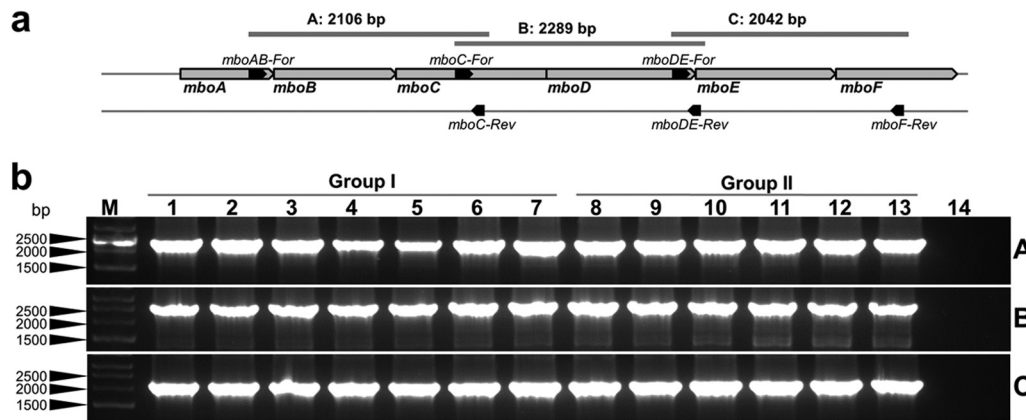
FIG 7 Internal organization of the *mbo* operon. (a) Schematic diagrams of the overlapping primers used for determining the organization of the *mbo* operon. The size of each amplicon is also shown. (b) Results of amplification in the selected strains belonging to groups I and II. *P. syringae* pv. syringae B728a (a non-mangotoxin producer) was included as a negative control. Lanes correspond to the following: 1, *P. syringae* pv. syringae 7C6; 2, *P. syringae* pv. syringae DAR77787; 3, *P. syringae* pv. syringae EPS17A; 4, *P. syringae* pv. syringae NCPPB1239; 5, *P. syringae* pv. syringae UMAF4002; 6, *P. syringae* pv. syringae UMAF0167; 7, *P. syringae* pv. syringae UMAF0158; 8, *P. syringae* pv. aptata DSM50252; 9, *P. syringae* pv. avellanae ISPaVe2056; 10, *P. syringae* pv. pisi NCPPB1365; 11, *P. syringae* pv. syringae 1444-5; 12, *P. syringae* pv. syringae FF5; 13, *P. syringae* pv. syringae CFBP3388; 14, *P. syringae* pv. syringae B728a; M, molecular size marker (HyperLadder I, Bioline).

that three strains of pathovar aptata produced an antimetabolite toxin inhibiting the arginine/ornithine biosynthesis pathway (51). However, the enzymatic step(s) affected could not be identified because the reversion of inhibition with purified amino acids followed an atypical pattern, suggesting the production of more than one antimetabolite toxin or of a toxin inhibiting different enzymatic steps. Additionally, transformants of strains FF5 and UMAF0167 that contained the *mbo* operon were able to produce mangotoxin in the inhibition assay (15), suggesting that they do not contain any mutation outside the *mbo* operon that could prevent the biosynthesis or functionality of this toxin. Although we did not find premature stop codons in any of the coding DNA sequences of the *mbo* operon from the genomes of strains FF5 and DSM50252, it is still possible that these operons contain specific mutations that prevent the biosynthesis of an active toxin with respect to the operon in strain UMAF0158. This is not unlikely, because instances of nontoxigenic isolates containing a toxin biosynthesis cluster have already been described for *P. syringae* pathovars that produce phaseolotoxin or tabtoxin (2, 8, 26, 56).

To study the evolutionary history of the *mbo* operon, we performed independent phylogenetic analyses using diverse housekeeping genes, as well as the *mgoA* operon, which is essential for mangotoxin biosynthesis but is present in all examined *P. syringae* strains. All of these analyses were highly congruent and revealed the same major clades, which were in agreement with previous results of studies that used different combinations of housekeeping genes (19, 21, 57–59). In particular, strains of genomospecies 1 containing the *mbo* operon clustered in two well-defined groups that mirror the relative degree of host specialization found in *P. syringae* pv. syringae (60). From these, group I contains *P. syringae* pv. syringae strains that were mainly isolated from woody hosts, particularly mango, whereas group II is enriched in strains from herbaceous hosts belonging to diverse pathovars. An important inconsistency among the different phylogenetic trees was identified with respect to the branching order of groups I, II, and III (Fig. 4), which results in some uncertainty over the number of times that the *mbo* operon has been acquired by the strains of genom-

ospecies 1. This type of discrepancy is commonly found in phylogenetic analyses of *P. syringae* when using different housekeeping genes or even different genes from an operon from the *hrp* cluster, particularly for very closely related taxa, and has been interpreted to be a consequence of genetic exchange and recombination (21, 59, 61–63). Examination of the *mbo* operon insertion site offers further significant clues about its evolutionary history, in that the insertion site was the same for all the strains and in all cases was associated with the loss of a continuous 67-bp fragment that is ancestral to *P. syringae*. The possibility that the *mbo* operon was acquired by an ancestor of genomospecies 1 and later lost by the ancestor of group III is difficult to maintain because this loss implies the concomitant reacquisition of the 67-bp fragment. Therefore, the simplest explanation implies that the *mbo* operon was acquired by a putative ancestor of groups I and II and has since evolved separately within both groups. Nevertheless, we cannot discount the less likely possibility that the operon was acquired by the ancestor of one of these two groups and then horizontally transferred to the ancestor of the other group, where the operon evolved independently. However, we could predict a very limited lateral transfer of the *mbo* operon because it is not linked to integrases, transposon sequences, or any other obvious repeated sequences; in contrast, the phaseolotoxin biosynthesis cluster from *P. syringae* pv. phaseolicola and *P. syringae* pv. actinidae is associated with integrases, which probably mediated its horizontal exchange between these two pathovars (13, 20, 64). This would suggest that the *mbo* operon was acquired by illegitimate recombination, a process that was shown to operate during the diversification of effector genes in *P. syringae* (65) but is predicted to occur with a very low frequency (66), further supporting the single-acquisition-event hypothesis.

In conclusion, the specificity of the *mbo* operon has allowed the design of specific primers and a PCR protocol that permits a fast and efficient method for identifying potential mangotoxin-producing strains. With this PCR method, we have detected the presence of the *mbo* operon in five pathovars of *P. syringae* from geno-

mospecies 1, whereas mangotoxin production has been reported for the first time in *P. syringae* pv. pisi. The high conservation of the structure, sequence, and genomic location of the *mbo* operon, together with the phylogenetic analysis showing that the *mbo* operon is present in only two groups from genomospecies 1 of the *P. syringae* complex, strongly suggests that the *mbo* operon has been horizontally acquired only once during the evolution of this bacterial species.

ACKNOWLEDGMENTS

REFERENCES

1. **Bender CL, Alarcón-Chaidez F, Gross DC.** 1999. *Pseudomonas syringae* phytotoxins: mode of action, regulation, and biosynthesis by peptide and polyketide synthetases. Microbiol. Mol. Biol. Rev. **63**:266–292.
2. **Gutiérrez-Barranquero JA, Arrebola E, Bonilla N, Sarmiento D, Cazorla FM, de Vicente A.** 2012. Environmentally friendly treatment alternatives to Bordeaux mixture for controlling bacterial apical necrosis (BAN) of mango. Plant Pathol. **61**:665–676.
3. **Kennelly MM, Cazorla FM, de Vicente A, Ramos C, Sundin GW.** 2007. *Pseudomonas syringae* diseases of fruit trees: progress toward understanding and control. Plant Dis. **91**:4–17.
4. **Krieg NR, Holt JG.** 1984. Bergey's manual of systematic bacteriology, vol 1. Williams & Wilkins, Baltimore, MD.
5. **Mansfield J, Genin S, Magori S, Citovsky V, Sriariyanum M, Ronald P, Dow M, Verdier V, Beer SV, Machado MA, Toth I, Salmond G, Foster GD.** 2012. Top 10 plant pathogenic bacteria in molecular plant pathology. Mol. Plant Pathol. **13**:614–629.
6. **Mansfield JW.** 2009. From bacterial avirulence genes to effector functions via the hrp delivery system: an overview of 25 years of progress in our understanding of plant innate immunity. Mol. Plant Pathol. **10**:721–734.
7. **Ramos C, Matas IM, Bardaji L, Aragón IM, Murillo J.** 2012. *Pseudomonas savastanoi* pv. savastanoi: some like it knot. Mol. Plant Pathol. **13**:998–1009.
8. **Arrebola E, Cazorla FM, Codina JC, Gutiérrez-Barranquero JA, Pérez-García A, de Vicente A.** 2009. Contribution of mangotoxin to the virulence and epiphytic fitness of *Pseudomonas syringae* pv. syringae. Int. Microbiol. **12**:87–95.
9. **Arrebola E, Cazorla FM, Pérez-García A, de Vicente A.** 2011. Chemical and metabolic aspects of antimetabolite toxins produced by *Pseudomonas syringae* pathovars. Toxins **3**:1089–1110.
10. **Arrebola E, Cazorla FM, Pérez-García A, de Vicente A.** 2011. Genes involved in the production of antimetabolite toxins by *Pseudomonas syringae* pathovars. Genes **2**:640–660.
11. **Arrebola E, Cazorla FM, Durán VE, Rivera E, Olea F, Codina JC, Pérez-García A, de Vicente A.** 2003. Mangotoxin: a novel antimetabolite toxin produced by *Pseudomonas syringae* inhibiting ornithine/arginine biosynthesis. Physiol. Mol. Plant Pathol. **63**:117–127.
12. **Arrebola E, Cazorla FM, Romero D, Pérez-García A, de Vicente A.** 2007. A nonribosomal peptide synthetase gene (*mgoA*) of *Pseudomonas syringae* pv. syringae is involved in mangotoxin biosynthesis and is required for full virulence. Mol. Plant-Microbe Interact. **20**:500–509.
13. **Murillo J, Bardaji L, Navarro de la Fuente L, Führer ME, Aguilera S, Álvarez-Morales A.** 2011. Variation in conservation of the cluster for biosynthesis of the phytotoxin phaseolotoxin in *Pseudomonas syringae*
14. **Arrebola E, Carrión VJ, Cazorla FM, Pérez-García A, Murillo J, de Vicente A.** 2012. Characterisation of the *mgo* operon in *Pseudomonas syringae* pv. *syringae* UMAF0158 that is required for mangotoxin production. BMC Microbiol. **12**:10. doi:10.1186/1471-2180-12-10.
15. **Carrión VJ, Arrebola E, Cazorla FM, Murillo J, de Vicente A.** 2012. The *mbo* operon is specific and essential for biosynthesis of mangotoxin in *Pseudomonas syringae*. PLoS One **7**:e36709. doi:10.1371/journal.pone.0036709.
16. **Rees-George J, Vanneste JL, Cornish DA, Pushparajah IPS, Yu J, Templeton MD, Everett KR.** 2010. Detection of *Pseudomonas syringae* pv. actinidiae using polymerase chain reaction (PCR) primers based on the 16S-23S rDNA intertranscribed spacer region and comparison with PCR primers based on other gene regions. Plant Pathol. **59**:453–464.
17. **Ercolani GL.** 1985. The relation between dosage, bacterial growth and time for disease response during infection of bean leaves by *Pseudomonas syringae* pv. phaseolicola. J. Appl. Microbiol. **58**:63–75.
18. **Penyalver R, García A, Ferrer A, Bertolini E, López MM.** 2000. Detection of *Pseudomonas savastanoi* pv. savastanoi in olive plants by enrichment and PCR. Appl. Environ. Microbiol. **66**:2673–2677.
19. **Sawada H, Suzuki F, Matsuda I, Saitou N.** 1999. Phylogenetic analysis of *Pseudomonas syringae* pathovars suggests the horizontal gene transfer of *argK* and the evolutionary stability of *hrp* gene cluster. J. Mol. Evol. **49**:627–644.
20. **Sawada H, Kanaya S, Tsuda M, Suzuki F, Azegami K, Saitou N.** 2002. A phylogenomic study of the OCTase genes in *Pseudomonas syringae* pathovars: the horizontal rransfer of the *argK*-tox cluster and the evolutionary history of OCTase genes on their genomes. J. Mol. Evol. **54**:437–457.
21. **Baltrus DA, Nishimura MT, Romanchuk A, Chang JH, Mukhtar MS, Cherkis K, Roach J, Grant SR, Jones CD, Dangl JL.** 2011. Dynamic evolution of pathogenicity revealed by sequencing and comparative genomics of 19 *Pseudomonas syringae* isolates. PLoS Pathog. **7**:e1002132. doi:10.1371/journal.ppat.1002132.
22. **Green S, Studholme DJ, Laue BE, Dorati F, Lovell H, Arnold D, Cottrell JE, Bridgett S, Blaxter M, Huitema E, Thwaites R, Sharp PM, Jackson RW, Kamoun S.** 2010. Comparative genome analysis provides insights into the evolution and adaptation of *Pseudomonas syringae* pv. aesculi on *Aesculus hippocastanum*. PLoS One **5**:e10224. doi:10.1371/journal.pone.0010224.
23. **Yamamoto S, Kasai H, Arnold DL, Jackson RW, Vivian A, Harayama S.** 2000. Phylogeny of the genus *Pseudomonas*: intrageneric structure reconstructed from the nucleotide sequences of *gyrB* and *rpoD* genes. Microbiology **146**:2385–2394.
24. **Reinhardt JA, Baltrus DA, Nishimura MT, Jeck WR, Jones CD, Dangl JL.** 2009. De novo assembly using low-coverage short read sequence data from the rice pathogen *Pseudomonas syringae* pv. oryzae. Genome Res. **19**:294–305.
25. **Teverson DM.** 1991. Genetics of pathogenicity and resistance in the haloblight disease of beans in Africa. Ph.D. thesis. University of Birmingham, Birmingham, United Kingdom.
26. **Rico A, López R, Asensio C, Aizpún MT, Asensio-S-Manzanera MC, Murillo J.** 2003. Nontoxigenic strains of *Pseudomonas syringae* pv. phaseolicola are a main cause of halo blight of beans in Spain and escape current detection methods. Phytopathology **93**:1553–1559.
27. **Pérez-Martínez I, Rodriguez-Moreno L, Matas IM, Ramos C.** 2007. Strain selection and improvement of gene transfer for genetic manipulation of *Pseudomonas savastanoi* isolated from olive knots. Res. Microbiol. **158**:60–69.
28. **Sundin GW, Bender CL.** 1996. Dissemination of the *strA-strB* streptomycin-resistance genes among commensal and pathogenic bacteria from humans, animals, and plants. Mol. Ecol. **5**:133–143.
29. **Sundin GW, Demezas DH, Bender CL.** 1994. Genetic and plasmid diversity within natural populations of *Pseudomonas syringae* with various exposures to copper and streptomycin bactericides. Appl. Environ. Microbiol. **60**:4421–4431.
30. **Feil H, Feil WS, Chain P, Larimer F, DiBartolo G, Copeland A, Lykidis A, Trong S, Nolan M, Goltsman E, Thiel J, Malfatti S, Loper JE, Lapidus A, Detter JC, Land M, Richardson PM, Kyrpides NC, Ivanova N, Lindow SE.** 2005. Comparison of the complete genome sequences of *Pseudomonas syringae* pv. syringae B728a and pv. tomato DC3000. Proc. Natl. Acad. Sci. U. S. A. **102**:11064–11069.

suggests at least two events of horizontal acquisition. Res. Microbiol. **162**:253–261.

31. **Tourte C, Manceau C.** 1995. A strain of *Pseudomonas syringae* which does not belong to pathovar phaseolicola produces phaseolotoxin. Eur. J. Plant Pathol. **101**:483–490.

32. **Martín-Sanz A, Palomo J, Pérez de la Vega M, Caminero C.** 2012. Characterization of *Pseudomonas syringae* pv. syringae isolates associated with bacterial blight in *Lathyrus* spp. and sources of resistance. Eur. J. Plant Pathol. **134**:205–216.

33. **Young A.** 2008. Notes on *Pseudomonas syringae* pv. syringae bacterial necrosis of mango (*Mangifera indica*) in Australia. Australas. Plant Dis. Notes **3**:138–140.

34. **Sohn KH, Jones JDG, Studholme DJ.** 2012. Draft genome sequence of *Pseudomonas syringae* pathovar syringae strain FF5, causal agent of stem tip dieback disease on ornamental pear. J. Bacteriol. **194**:3733–3734.

35. **Martín-Sanz A, Palomo JL, Caminero C.** 2009. First report of bacterial blight caused by *Pseudomonas syringae* pv. *syringae* on common vetch in Spain. Plant Dis. **93**:1348.

36. **Cazorla FM, Arrebola E, Sesma A, Pérez-García A, Codina JC, Murillo J, de Vicente A.** 2002. Copper resistance in *Pseudomonas syringae* strains isolated from mango is encoded mainly by plasmids. Phytopathology **92**:909–916.

37. **Gutiérrez-Barranquero JA, Arrebola E, Pérez-García A, Codina JC, Murillo J, de Vicente A, Cazorla FM.** 2008. Evaluation of phenotypic and genetic techniques to analyze diversity of *Pseudomonas syringae* pv. syringae strains isolates from mango trees, p 271–281. *In* Fatmi MB, Collmer A, Iacobellis NS, Mansfield JW, Murillo J, Schaad NW, Ullrich M (ed), *Pseudomonas syringae* pathovars and related pathogens—identification, epidemiology and genomics. Springer Netherlands, Dordrecht, The Netherlands.

38. **Moore RA, Starratt AN, Ma SW, Morris VL, Cuppels DA.** 1989. Identification of a chromosomal region required for biosynthesis of the phytotoxin coronatine by *Pseudomonas syringae* pv. tomato. Can. J. Microbiol. **35**:910–917.

39. **Cai R, Lewis J, Yan S, Liu H, Clarke CR, Campanile F, Almeida NF, Studholme DJ, Lindeberg M, Schneider D, Zaccardelli M, Setubal JC, Morales-Lizcano NP, Bernal A, Coaker G, Baker C, Bender CL, Leman S, Vinatzer BA.** 2011. The plant pathogen *Pseudomonas syringae* pv. tomato is genetically monomorphic and under strong selection to evade tomato immunity. PLoS Pathog. **7**:e1002130. doi:10.1371/journal.ppat.1002130.

40. **Almeida NF, Yan S, Lindeberg M, Studholme DJ, Schneider DJ, Condon B, Liu H, Viana CJ, Warren A, Evans C, Kemen E, MacLean D, Angot A, Martin GB, Jones JD, Collmer A, Setubal JC, Vinatzer BA.** 2008. A draft genome sequence of *Pseudomonas syringae* pv. tomato T1 reveals a type III effector repertoire significantly divergent from that of *Pseudomonas syringae* pv. tomato DC3000. Mol. Plant-Microbe Interact. **22**:52–62.

41. **Sambrook J, Russell DW.** 2001. Molecular cloning: a laboratory manual, 3rd ed, vol 1. Cold Spring Harbor Laboratory Press, Cold Spring Harbor, NY.

42. **King EO, Ward MK, Raney DE.** 1954. Two simple media for the demonstration of pyocyanin and fluorescein. J. Lab. Clin. Med. **44**:301–307.

43. **Cazorla FM, Olalla L, Torés JA, Codina JC, Pérez-GarcíA A, de Vicente A.** 1997. *Pseudomonas syringae* pv. syringae as microorganism involved in apical necrosis of mango: characterization of some virulence factors, p 82–87. *In* Rudolph K, Burr TJ, Mansfield JW, Stead D, Vivian A, von Kietzell J (ed), *Pseudomonas syringae* pathovars and related pathogens. Kluwer Academic Publishers, Dordrecht, The Netherlands.

44. **Gasson MJ.** 1980. Indicator technique for antimetabolic toxin production by phytopathogenic species of *Pseudomonas*. Appl. Environ. Microbiol. **39**:25–29.

45. **Rozen S, Skaletsky H.** 2000. Primer3 on the WWW for general users and for biologist programmers. Methods Mol. Biol. **132**:365–386.

46. **Altschul SF, Gish W, Miller W, Myers EW, Lipman DJ.** 1990. Basic local alignment search tool. J. Mol. Biol. **215**:403–410.

47. **Rutherford K, Parkhill J, Crook J, Horsnell T, Rice P, Rajandream M-A, Barrell B.** 2000. Artemis: sequence visualization and annotation. Bioinformatics **16**:944–945.

48. **Carver TJ, Rutherford KM, Berriman M, Rajandream M-A, Barrell BG, Parkhill J.** 2005. ACT: the Artemis comparison tool. Bioinformatics **21**:3422–3423.

49. **Abbott JC, Aanensen DM, Rutherford K, Butcher S, Spratt BG.** 2005. WebACT—an online companion for the Artemis comparison tool. Bioinformatics **21**:3665–3666.

50. **Tamura K, Peterson D, Peterson N, Stecher G, Nei M, Kumar S.** 2011. MEGA5: molecular evolutionary genetics analysis using maximum likelihood, evolutionary distance, and maximum parsimony methods. Mol. Biol. Evol. **28**:2731–2739.

51. **Völksch B, Weingart H.** 1998. Toxin production by pathovars of *Pseudomonas syringae* and their antagonistic activities against epiphytic microorganisms. J. Basic Microbiol. **38**:135–145.

52. **Gardan L, Shafik H, Belouin S, Broch R, Grimont F, Grimont PAD.** 1999. DNA relatedness among the pathovars of *Pseudomonas syringae* and description of *Pseudomonas tremae* sp. nov. and *Pseudomonas cannabina* sp. nov. (*ex* Sutic and Dowson 1959). Int. J. Syst. Bacteriol. **49**:469–478.

53. **Buell CR, Joardar V, Lindeberg M, Selengut J, Paulsen IT, Gwinn ML, Dodson RJ, Deboy RT, Durkin AS, Kolonay JF, Madupu R, Daugherty S, Brinkac L, Beanan MJ, Haft DH, Nelson WC, Davidsen T, Zafar N, Zhou L, Liu J, Yuan Q, Khouri H, Fedorova N, Tran B, Russell D, Berry K, Utterback T, Van Aken SE, Feldblyum TV, D'Ascenzo M, Deng W-L, Ramos AR, Alfano JR, Cartinhour S, Chatterjee AK, Delaney TP, Lazarowitz SG, Martin GB, Schneider DJ, Tang X, Bender CL, White O, Fraser CM, Collmer A.** 2003. The complete genome sequence of the *Arabidopsis* and tomato pathogen *Pseudomonas syringae* pv. tomato DC3000. Proc. Natl. Acad. Sci. U. S. A. **100**:10181–10186.

54. **Martín-Sanz A, Pérez de la Vega M, Murillo J, Caminero C.** 2012. Genetic, biochemical and pathogenic diversity of *Pseudomonas syringae* pv. *pisi* strains. Plant Pathol. **61**:1063–1072.

55. **Cazorla FM, Torés JA, Olalla L, Pérez-García A, Farré JM, de Vicente A.** 1998. Bacterial apical necrosis of mango in southern Spain: a disease caused by *Pseudomonas syringae* pv. *syringae*. Phytopathology **88**:614–620.

56. **Schaad NW, Cheong SS, Tamaki S, Hatziloukas E, Panopoulos NJ.** 1995. A combined biological and enzymatic amplification (BIO-PCR) technique to detect *Pseudomonas syringae* pv. phaseolicola in bean seed extracts. Phytopathology **85**:243–248.

57. **Gironde S, Manceau C.** 2012. Housekeeping gene sequencing and multilocus variable-number tandem-repeat analysis to identify subpopulations within *Pseudomonas syringae* pv. maculicola and *Pseudomonas syringae* pv. tomato that correlate with host specificity. Appl. Environ. Microbiol. **78**:3266–3279.

58. **Hwang MS, Morgan RL, Sarkar SF, Wang PW, Guttman DS.** 2005. Phylogenetic characterization of virulence and resistance phenotypes of *Pseudomonas syringae*. Appl. Environ. Microbiol. **71**:5182–5191.

59. **Sarkar SF, Guttman DS.** 2004. Evolution of the core genome of *Pseudomonas syringae*, a highly clonal, endemic plant pathogen. Appl. Environ. Microbiol. **70**:1999–2012.

60. **Little EL, Bostock RM, Kirkpatrick BC.** 1998. Genetic characterization of *Pseudomonas syringae* pv. syringae strains from stone fruits in California. Appl. Environ. Microbiol. **64**:3818–3823.

61. **Guttman DS, Gropp SJ, Morgan RL, Wang PW.** 2006. Diversifying selection drives the evolution of the type III secretion system pilus of *Pseudomonas syringae*. Mol. Biol. Evol. **23**:2342–2354.

62. **Wang PW, Morgan RL, Scortichini M, Guttman DS.** 2007. Convergent evolution of phytopathogenic pseudomonads onto hazelnut. Microbiology **153**:2067–2073.

63. **Yan S, Liu H, Mohr TJ, Jenrette J, Chiodini R, Zaccardelli M, Setubal JC, Vinatzer BA.** 2008. Role of recombination in the evolution of the model plant pathogen *Pseudomonas syringae* pv. tomato DC3000, a very atypical tomato strain. Appl. Environ. Microbiol. **74**:3171–3181.

64. **Genka H, Baba T, Tsuda M, Kanaya S, Mori H, Yoshida T, Noguchi M, Tsuchiya K, Sawada H.** 2006. Comparative analysis of argK-tox clusters and their flanking regions in phaseolotoxin-producing *Pseudomonas syringae* pathovars. J. Mol. Evol. **63**:401–414.

65. **Stavrinides J, Ma W, Guttman DS.** 2006. Terminal reassortment drives the quantum evolution of type III effectors in bacterial pathogens. PLoS Pathog. **2**:e104. doi:10.1371/journal.ppat.0020104.

66. **Thomas CM, Nielsen KM.** 2005. Mechanisms of, and barriers to, horizontal gene transfer between bacteria. Nat. Rev. Microbiol. **3**:711–721.